The effect of Nd and Mg doping on the micro-Raman spectra of $LiNbO_3$ single-crystals

2009 J. Phys.: Condens. Matter 21 145401

(http://iopscience.iop.org/0953-8984/21/14/145401)

J. Phys.: Condens. Matter **21** (2009) 145401 (7pp) doi:10.1088/0953-8984/21/14/145401

The effect of Nd and Mg doping on the micro-Raman spectra of $LiNbO_3$ single-crystals

R Quispe-Siccha[1], E V Mejía-Uriarte[2], M Villagrán-Muniz[1], D Jaque[3], J García Solé[3], F Jaque[3], R Y Sato-Berrú[4], E Camarillo[5], J Hernández A[5] and H Murrieta S[5]

[1] Laboratorio de Fotofísica, Centro de Ciencias Aplicadas y Desarrollo Tecnológico, Universidad Nacional Autónoma de México, AP 70-186, DF, Mexico
[2] Laboratorio de Fotónica de Microondas, Centro de Ciencias Aplicadas y Desarrollo Tecnológico, Universidad Nacional Autónoma de México, AP 70-186, DF, Mexico
[3] Laboratorio de Espectroscopia Láser, Departamentode Física de Materiales, Universidad Autónoma de Madrid, Madrid 28049, Spain
[4] Laboratorio de Materiales y Nanotecnología, Centro de Ciencias Aplicadas y Desarrollo Tecnológico, Universidad Nacional Autónoma de México, AP 70-186, DF, Mexico
[5] Laboratorio Propiedades Ópticas, Instituto de Física, Universidad Nacional Autónoma de México, AP 20-364, Mexico

E-mail: rosa.quispe@gmail.com, elsi.mejia@ccadet.unam.mx, mayo.villagran@ccadet.unam.mx, dani.jaque@uam.es, jose.garcia_sole@uam.es, francisco.jaque@uam.es, roberto.sato@ccadet.unam.mx, cgarcia@fisica.unam.mx, josemh@fisica.unam.mx and murrieta@fisica.unam.mx

Received 24 November 2008, in final form 17 January 2009
Published 5 March 2009
Online at stacks.iop.org/JPhysCM/21/145401

Abstract
The $LiNbO_3$ congruent crystals doped with small Nd concentrations, <1 mol% Nd, and co-doped with Mg ions, 0–9 mol% Mg, were systematically investigated by means of micro-Raman spectroscopy in the *Y* and *Z* crystal directions. Results obtained from an undoped congruent crystal, an Nd-doped crystal, a Mg-doped crystal and Nd, Mg-co-doped crystals are compared. From the analyses of the results obtained in the *Y* direction, the Nd and Mg content dependence of the two lowest-Raman $A_1(TO_1)$ and $A_1(TO_2)$ modes, the half-width composition and the area ratio of the $A_1(TO_4)$ and $E(TO_8)$ bands, we reached several conclusions about the incorporation mechanism of the Nd and Mg ions into the $LiNbO_3$ lattice. Likewise the Raman shift and half-width of the $E(TO_1)$ and $E(TO_7)$ modes were investigated in the *Z* direction. Results indicate that Mg and Nd ions are located in the Li site for low doping concentrations and for larger concentrations there is a replacement in both Li and Nb ion sites.

1. Introduction

There has been a growing interest in the fundamental role of the neodymium impurity ions in $LiNbO_3$ (LN) crystals when used as a laser-ion host; however, it has limited use due to the photorefractive damage. It has been observed that the addition of 5% or more of MgO in $LiNbO_3$ greatly reduces this damage [1, 2], but it also influences other things such as the Nd^{3+} ion distribution into different crystal sites [3–5].

Currently it is known [6] that the Nd^{3+} ions are occupying several non-equivalent sites (different local environment) in the crystal, thus giving place to different Nd^{3+} optical centers. However, the knowledge of the lattice location of the impurities as well as its symmetry and local environment are needed for an understanding of microscopic processes induced by the impurity doping. Site locations of the Nd ions in LN crystals were investigated by optical spectroscopy under laser pumping (laser spectroscopy, LS) and channeled Rutherford backscattering (RBS) [6, 7]. The investigation found that Nd ions occupy three different off-centered Li crystal sites. An additional center was detected in LN:Nd crystals co-doped

with Mg. Channeling experiments confirmed that rare-earth (RE^{3+}) ions are located in Li octahedral sites, but off-center from the regular Li position, relaxed towards the nearest oxygen plane by about 0.4 Å.

Since the sensitivity of the Raman spectrum depends on the changes in composition and the amount of doping materials, it can be used to investigate the incorporation of Nd and Mg ions into the $LiNbO_3$ crystal lattice. The frequencies of phonon modes for both A_1 and E symmetries in the LN lattice have been clearly established from Raman scattering measurements on a stoichiometric crystal (i.e. 50 mol% LiO_2 and 50 mol% Nb_2O_5) [8, 9]. The allocation of each phonon mode to a particular displacement of ions was achieved only very recently by Caciuc *et al* [10] and the problem of exact assignment between all vibrational modes and the Raman bands was solved recently by Ridah *et al* [11, 12].

Despite many studies, the defects of the Mg-doped $LiNbO_3$ crystal structure in congruent and stoichiometric composition is still an unsolved question and has been generally discussed on the basis of a defect model in the undoped crystal, which is always the subject of controversies [11–13]. The Li-deficient lattice can be thus described generally in terms of Li vacancies [11, 12] or Nb vacancies [13] according to different charge compensation mechanisms. Using the Raman spectroscopy technique, some authors [11, 14–17] worked on the Mg doping mechanism, indicating the location of the Mg ions for low and large Mg concentrations in LN crystals with congruent and stoichiometric compositions. Mouras *et al* [18] worked on the location of rare-earth ions in $LiNbO_3$ crystals and recently, Donnerberg [19] stated that a realistic description would be independent of a particular model for intrinsic defects.

The present study deals with the experimental characterization of Nd and Mg ions' incorporation into the LN lattice using Raman scattering measurements, which provide a direct probe site, compared to other techniques used in earlier studies. The assignment of the $A_1(TO_1)$, $A_1(TO_2)$, $E(TO_8)$ and $A_1(TO_4)$ modes, in the Y direction of the crystals and the $E(TO_1)$ and $E(TO_7)$ modes in the Z direction were used to interpret the changes of the Raman spectrum in terms of the defect substitution model.

2. Experimental details

The single-crystals used in this work were grown at the Universidad Autónoma de Madrid, by the Czochralski method, with congruent composition in the melt, Li/Nb = 0.945. The single LN crystals containing different amounts of neodymium and magnesium ions used in this work were: $LiNbO_3$-pure, Nd-doped (0.28 mol%), Nd:Mg-doped (0.21 mol%, 3 mol%), Mg-doped (5 mol%), Nd:Mg-doped (0.07 mol%, 6 mol%), Nd:Mg-doped (0.19 mol%, 8 mol%) and Nd:Mg-doped (0.08 mol%, 9 mol%). It should be noticed that an initial amount of Nd 1 mol% was added to the melt; its final concentrations were determined by x-ray fluorescence spectrometry. The Mg concentration is just the amount added to the melt. The samples were prepared in the Y- and Z-cut and their faces were carefully polished with diamond powder of 1/4 μm. Raman spectra were recorded with a Raman dispersive spectrometer, model Almega XR. An Olympus microscope (BX51) and an Olympus 50× objective (NA = 0.80) were used for focusing the laser on the sample using a spot size of ∼1 μm, and for collecting the scattered light in a 180° backscattering configuration. The Raman spectra were accumulated over 25 s with a resolution of ∼4 cm^{-1} and the excitation source was 532 nm radiation from an Nd:YVO_4 laser (frequency-doubled). The Raman scattering measurement in the Y direction of the single-crystals was chosen because it is suitable for providing the closed $A_1(TO_1, TO_2)$ phonons and also the $E(TO_8)$–$A_1(TO_4)$ phonons. The Z direction of the single-crystals was chosen for analysis of the behavior of the vibrations of Nb/O in the $E(TO_1)$ mode and the vibrations of Li/O in the $E(TO_7)$ mode.

3. Results and discussions

Figures 1 and 4 show the Raman spectrum of seven single-crystals doped with different amounts of Nd and Mg ions, recorded in the Y and Z directions of the samples. The analyzed modes in this work, according to the normal modes calculated by Caciuc *et al* [10], correspond to the $E(TO_1, TO_3)$ and $A_1(TO_1)$ modes that match the Nb/O vibrations. The $A_1(TO_2)$ mode mainly involves Li/Nb motions, whereas the $A_1(TO_4)$ and $E(TO_8)$ modes correspond to the stretching vibration of the oxygen octahedron (O/O). The $E(TO_7)$ mode corresponds to the Li/O vibrations. The analyses of these modes can be seen in figures 2, 3 and 5.

3.1. Raman modes in Nd, Mg-doped congruent single-crystals

The Raman spectra in the Y direction, for different impurity concentrations, are shown in figure 1(a). According to Lengyel [14] they correspond to the sum of two $y(zx)y$ and $y(zz)y$ configurations. The $E(TO_3)$ mode and the two $A_1(TO_1)$ and $A_1(TO_2)$ modes, displayed in figure 1(b), are lying close to each other at about 235.24 cm^{-1} for $E(TO_3)$, 255.91 cm^{-1} for $A_1(TO_1)$ and 273 cm^{-1} for $A_1(TO_2)$ in the undoped congruent single-crystal; to deduce each phonon frequency three damped harmonic oscillators are required to fit the spectrum. As the three modes are lying close to each other, the fitting of each is not an easy task. The most striking change is the wavenumber shift for the $A_1(TO_1)$ and $A_1(TO_2)$ modes rather than that for the $E(TO_3)$ mode, as can be seen in figure 1(b). The $A_1(TO_2)$ mode shows a large decrease of its wavenumber with the incorporation of Nd, Mg and by increasing (Mg + Nd) concentrations. The intensity of the peak $A_1(TO_2)$ appearing at 273 cm^{-1} in pure LN decreases as the concentration of (Mg + Nd) increases in LN samples. For an (8 mol% Mg + 0.19 mol% Nd)-concentration in $LiNbO_3$, this peak disappeared. The disappearance of the NbO_6-related $A_1(TO_2)$ internal vibrational mode is positive confirmation of the formation of (Mg_{Nb}) defects in heavily (Mg + Nd)-doped $LiNbO_3$, as was also discussed by Kim *et al* [20] for heavily Mg-doped $LiNbO_3$. The $A_1(TO_1)$ mode shows a large and monotonic decrease of its wavenumber with the incorporation of Nd, Mg and with the (Mg + Nd) content. These changes

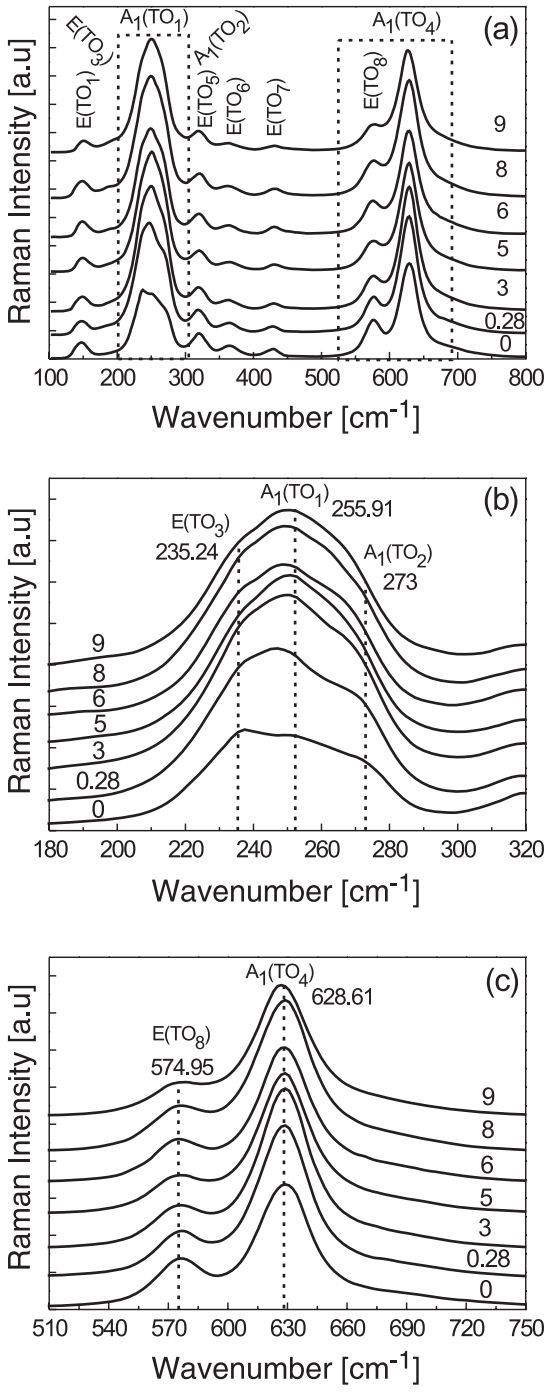

Figure 1. (a) Raman spectra recorded in the *Y* direction for LN-pure, LN:Nd(0.28), LN:Mg(5) and for different (Mg + Nd)-concentrations in single-crystals. (b) Enlargement of the $E(TO_3)$, $A_1(TO_1)$ and $A_1(TO_2)$ modes and (c) enlargement of the $E(TO_8)$ and $A_1(TO_4)$ modes. The figure is arranged as follows: [0] $LiNbO_3$; [0.28] $LiNbO_3$:Nd (0.28%); [3] $LiNbO_3$:Nd:Mg (0.21%, 3%); [5] $LiNbO_3$:Mg (5%); [6] $LiNbO_3$:Nd:Mg (0.07%, 6%); [8] $LiNbO_3$:Nd:Mg (0.19%, 8%); [9] $LiNbO_3$:Nd:Mg (0.08%, 9%).

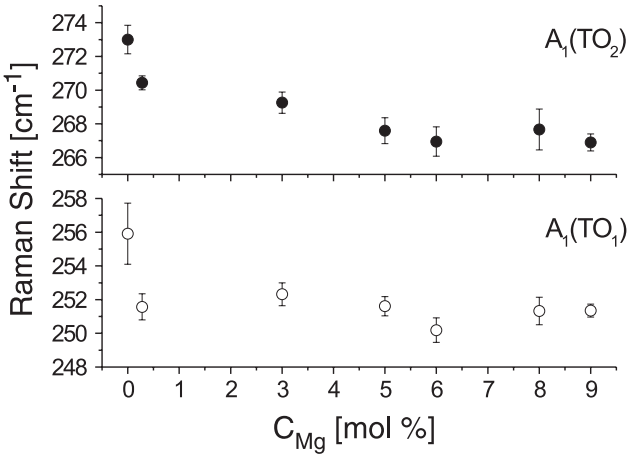

Figure 2. Nd, Mg and (Mg + Nd) concentration dependence of Raman shift for the $A_1(TO_1)$ and $A_1(TO_2)$ modes in the *Y* direction of the single-crystals.

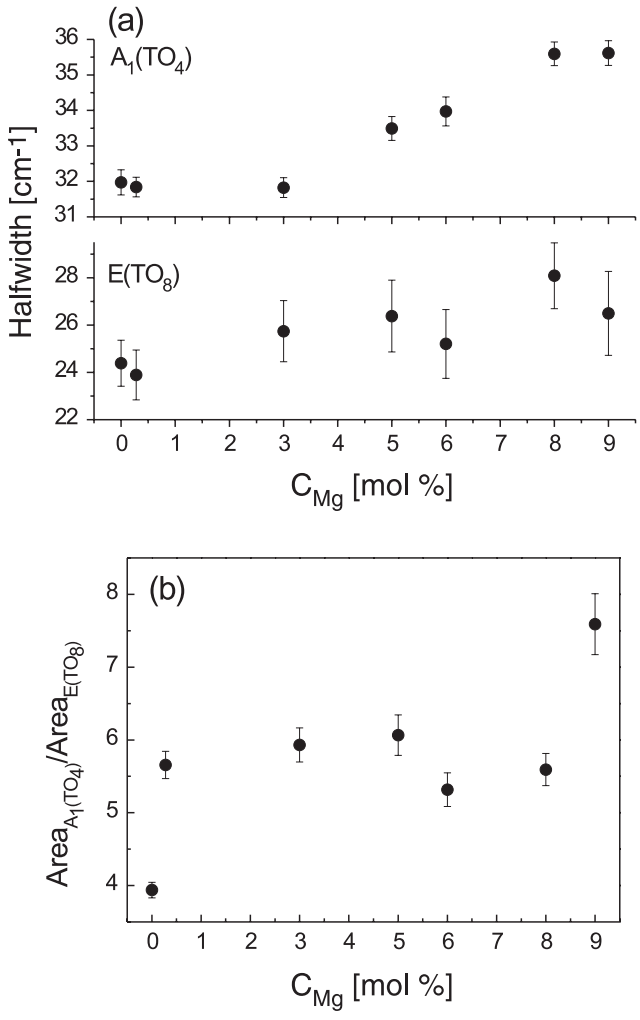

Figure 3. (a) Nd, Mg and (Nd + Mg) concentration dependence of half-width for the $A_1(TO_4)$ and $E(TO_8)$ modes. (b) Area ratio of the $A_1(TO_4)/E(TO_8)$ bands in the *Y* direction of the single-crystals.

are shown in figure 1(b). Results derived from these spectra adjustments are given in figure 2. These results are consistent with those of Mouras *et al* [21] for crystals doped with Mg ions.

The $E(TO_2)$ mode in the 177 cm^{-1}, $E(TO_4)$ mode in 262 cm^{-1} and the $E(TO_9)$ mode in 633 cm^{-1} are not shown in figure 1(a), since these are much less intense than the other modes [11]. The $A_1(TO_4)$ and $E(TO_8)$ modes appear to be only slightly affected by Nd and Mg doping. The

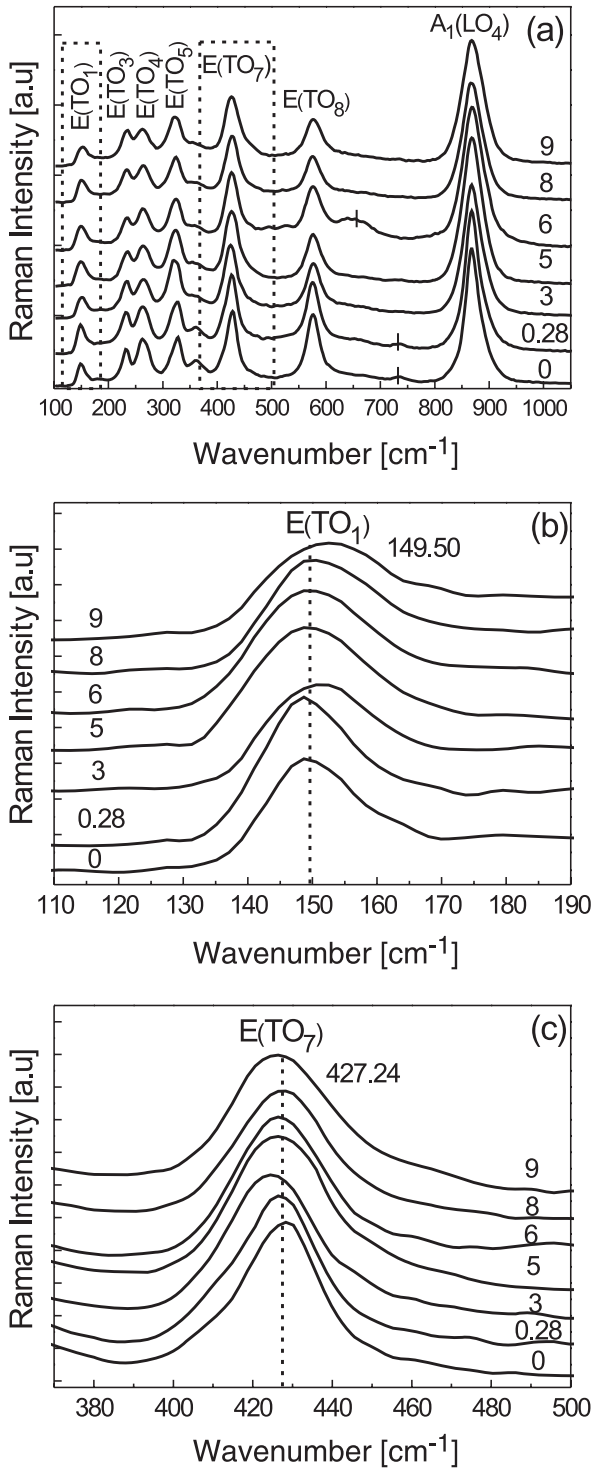

Figure 4. (a) Raman spectra recorded in the Z direction for LN-pure, LN:Nd(0.28), LN: Mg-5 and with different (Mg + Nd)-concentrations in the single-crystals. (b) Enlargement of the $E(TO_1)$ mode. (c) Enlargement of the $E(TO_7)$ mode. The figure is arranged as follows: [0] $LiNbO_3$; [0.28] $LiNbO_3$:Nd (0.28%); [3] $LiNbO_3$:Nd:Mg (0.21%, 3%); [5] $LiNbO_3$:Mg (5%); [6] $LiNbO_3$:Nd:Mg (0.07%, 6%); [8] $LiNbO_3$:Nd:Mg (0.19%, 8%); [9] $LiNbO_3$:Nd:Mg (0.08%, 9%).

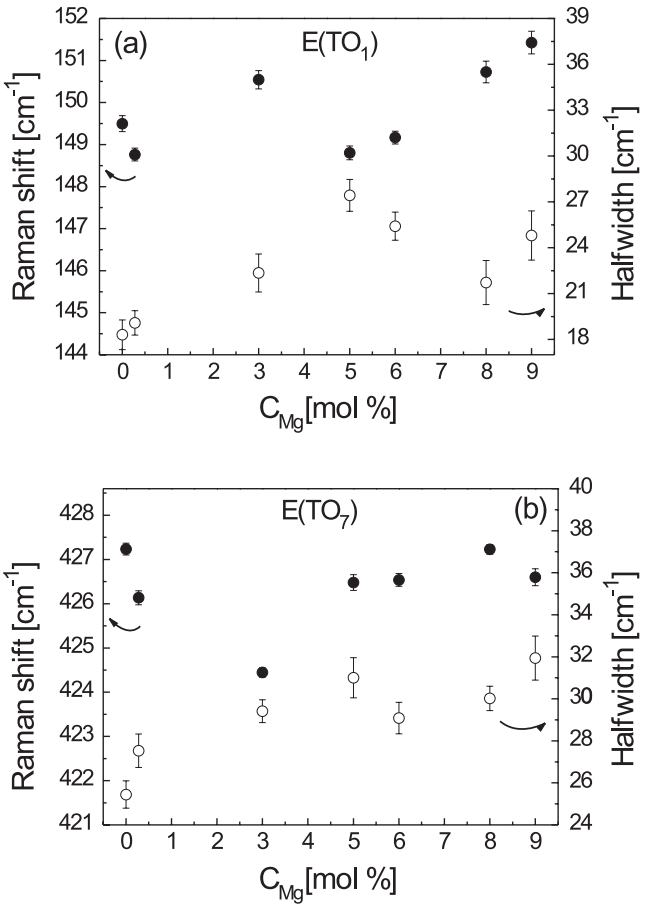

Figure 5. Nd, Mg and (Mg + Nd) concentration dependence of Raman shift and of half-width for the $E(TO_1)$ and $E(TO_7)$ modes in the Z direction of the single-crystals.

maximum positions of the $A_1(TO_4)$ and $E(TO_8)$ modes are not shifted, but for the $A_1(TO_4)$ band in high (Mg + Nd) content, for example, in the LN:Nd(0.08):Mg(9) sample, its position shows a slight shift to low wavenumbers by approximately 1.1 cm^{-1} as compared with the other samples. However, the half-width composition of the $A_1(TO_4)$ and $E(TO_8)$ modes present changes with the incorporations of Nd and Mg ions. The half-width composition of the $A_1(TO_4)$ mode presents a slight decrease with the incorporation of Nd(0.28) and LN:Nd(0.21):Mg(3) concentrations by approximately 0.13 cm^{-1} and 0.15 cm^{-1} respectively in relation to pure LN, while for high Mg and (Mg + Nd) content the half-width composition increases linearly. The two $E(TO_8)$ and $A_1(TO_4)$ bands are the result of the stretching vibrations of the oxygen octahedron, thus, when there is an increase of the half-width composition of the $A_1(TO_4)$ mode due to changes in the vibrational frequencies, the half-width composition of the $E(TO_8)$ mode also increases since it is affected by the closeness of the previously mentioned mode and not due to changes in the composition of the $E(TO_8)$ band, as can be seen in figure 1(b). Results derived from this spectra adjustment are given in figure 3(a), where it can be easily seen that within the experimental error the half-width remains constant.

The changes in the area ratio between the $A_1(TO_4)$ and $E(TO_8)$ bands can be interpreted as the contribution of the distortion of the oxygen octahedron when the Nd and Mg ions enter the LN lattice. The area of the $A_1(TO_4)$ band increases with the incorporation of Nd, Mg and (Mg + Nd) ions while

the area of the $E(TO_8)$ band remained approximately constant, as discussed above. As the $A_1(TO_4)$ band widens quickly it affects the $E(TO_8)$ band, which if anything moves very slowly. So if the $A_1(TO_4)$ band increases and the $E(TO_8)$ band remains approximately constant, the general tendency shown in figure 3(b) is that of an increase.

These features can be interpreted consistently with the predicted eigenvectors associated with the $E(TO_8)$ and $A_1(TO_4)$ modes, which exhibit the motion of oxygen ions only. Nd and Mg ions clearly do not substitute oxygen ions and their introduction in the lattice gives rise to a distortion of the oxygen octahedron and an anharmonic contribution to the vibrational modes.

The Raman spectrum, obtained with different concentrations, shows the $E(TO_1, TO_3–TO_8)$ modes and the $A_1(LO_4)$ longitudinal mode in the $z(xx)z$ in the Z direction of the single-crystal configuration, as can be seen in figure 4(a). These results are in agreement with those previously reported by Lengyel *et al* [14, 15]. The $E(TO_2, TO_9)$ bands are not discussed since they are much less intense than the other bands. In this configuration we analyzed the $E(TO_1)$ and $E(TO_7)$ modes at approximately 149.50 cm^{-1} and 427.24 cm^{-1} respectively; they are listed in figures 4(b) and (c).

The $E(TO_1)$ band changes with the incorporation of Nd, Mg and (Mg + Nd) ions. The changes are reflected as a wavenumber shift showing a monotonic increase as the Mg concentration increases, as can be seen in figure 4(b), and the results derived from this spectrum adjustment are shown in figure 5(a). The width of the Raman peaks indicates a disorder within the crystal structure. In particular, the width of the $E(TO_1)$ mode is especially interesting because it is thought to reflect the disorder in the Nb sub-lattice (assuming that oxygen sites are fully and normally occupied). The half-width composition of the $E(TO_1)$ mode increases approximately linearly with the Mg concentration. This increase is due to the disorder in the Nb sub-lattice induced by the competition of the Nd and Mg ions to occupy the Nb crystal sites, as seen in figure 4(b). The results derived from this spectrum adjustment are reported in figure 5(a).

The $E(TO_7)$ band is also affected by the incorporation of Nd, Mg and (Mg + Nd) ions, the LN:Nd(0.28) is shifted to lower wavenumber values by approximately 1.10 cm^{-1}, and the LN:Nd(0.21):Mg(3) by 2.79 cm^{-1} with respect to NL, but starting from 5 mol% Mg and higher Mg content there is a tendency to increase the wavenumber values. Previous studies have established linear dependences of the position of this Raman line as a function of the composition from congruence to stoichiometry [15]. The half-width composition in particular of the $E(TO_7)$ mode is especially interesting since it is thought to reflect the disorder in the Li sub-lattice (assuming that oxygen sites are fully and normally occupied). The half-width composition of the $E(TO_7)$ mode presents a general increase with the incorporation of Nd, Mg and (Mg + Nd) ions. This could be due to the disorder introduced in the Li sub-lattice by the competition of Nd and Mg ions for crystal sites within the lattice. This half-width increase is shown in figure 4(c) and analysis of the results derived from this spectra adjustment can be seen in figure 5(b).

3.2. Variation of the Raman parameters with Nd and Mg content

For a more quantitative determination of the band parameters, Lorentzian or damped oscillator functions were fitted to a number of spectra with their respective error bars. Therefore, a sum of Lorentzian functions was fitted to all Raman spectra. This method to adjust a number of spectra has been widely used in Raman spectroscopy [12, 14, 15, 17, 18, 20]. These results are interpreted below in terms of the Nd and Mg substitution process in the LN lattice, in light of the respective displacement patterns associated with $A_1(TO_1, TO_2, TO_4)$ and $E(TO_1, TO_4, TO_8)$ phonons and the area ratio of the $A_1(TO_4)/E(TO_8)$ bands.

The eigenvector patterns, as obtained by Postnikov *et al* [8], provide information about the kind of motion involved in a particular mode according to symmetry rules, but regardless of whether the site is occupied or not; this refers to the behavior of the oxygen vibrations around an Li vacancy that are going to be modified by the presence of the impurity ion located in that lattice site. Their results therefore can be used in the congruent LN lattice as well as in the doped LN crystal. This means that the $A_1(TO_1)$ and $E(TO_3)$ modes are mainly the vibration of ions in the Nb site with respect to oxygen ions, whereas the $A_1(TO_2)$ mode corresponds to the antiphase motion of ions in Li and Nb sites. The most important feature observed in this work is the large decrease of the $A_1(TO_2)$ Raman shift for the whole investigated (Nd, Mg and Nd + Mg) concentrations. As the TO_2 is the only mode which involves Li ion motion, this result can be related to Nd and Mg ions' introduction in the Li sites. As these sites can be occupied by Li ions, Li vacancies and/or Nb ions (the so-called antisites), the dependence of the $A_1(TO_2)$ Raman shift on the Nd and Mg concentration can be understood by successive processes within the Nd, Mg and (Mg + Nd) ions' substitution mechanism. Whatever the model proposed to describe the undoped crystal, vacant Li sites are occupied by Nb ions in the congruent LN lattice. Since they are particularly unstable, these positions should be, therefore, firstly affected by the Nd and Mg introduction. Under Nd, Mg doping, the Nd and Mg ions push Nb ions out of the antisites. Since the Nd mass is larger than the Mg mass and the Mg mass is larger than the Li mass, the continuous decrease of $A_1(TO_2)$ Raman shift can be related to the successive processes as follows: (i) the filling by Nd and Mg ions of Li vacancies and (ii) the partial replacement of Li ions in their proper sites.

This scenario is corroborated by the behavior of the $A_1(TO_1)$ and $E(TO_3)$ modes which consist of Nb vibration against oxygen ions. For low concentration, the decrease of $A_1(TO_1)$ frequency is not in contradiction with the fact that more Nb sites are occupied by Nb ions, which are pushed out from Li sites by Nd, Mg and (Mg + Nd) doping. For large (Mg + Nd) content, the increase of $A_1(TO_1)$ frequency reveals the substitution of Mg and Nd ions for Nb ions and thus reflects a change in the doping process. The positive sign of the Raman shift is in agreement with the respective masses of Nb and Mg. The explanation about the incorporation of Nd ions into both kinds of (Li and Nb) lattice sites has been suggested from the results obtained from EPR measurements [7], and from RBS/channeling experiments [22].

The analysis of the half-widths provides additional information related to the lattice vacancies and of the sites' environment. It is known that the substitution of ions by impurity defects is accompanied by charge compensation and therefore by local structural changes around the site. This can lead to a perturbation or disordering in the regular lattice, thus producing an increase in the line half-width. Therefore from the plots of the half-width, it is possible to deduce information related to the environment of Nd and Mg ions on both Li and Nb sites.

In particular, the width of $E(TO_8)$ and $A_1(TO_4)$ bands is especially interesting because they are related to the motion of oxygen anions only. The half-width composition of these modes changes with the incorporation of Mg and (Mg + Nd) ions, due to charge compensation and local structural changes around Nd and Mg sites. For the $E(TO_8)$ mode the half-width changes point to a perturbation or disordering of the regular lattice due to off-center Nd ions (located towards the nearest oxygen plane).

The changes in the area ratio of the $A_1(TO_4)/E(TO_8)$ modes is a consequence of the strong sensitivity of the lattice sites of the $LiNbO_3$ crystal to the incorporation of Nd and Mg ions, which, for example, affect the oxygen–oxygen stretching vibrations in a different way. The incorporation of Nd and Mg ions within the lithium niobate lattice gives rise to a distortion of the oxygen octahedron, and an anharmonic contribution to the vibrational modes due to their different mass, ionic radii and Nd ions located off-center from the regular Li position displaced towards the nearest oxygen plane. This distortion produces the area increases of the $A_1(TO_4)$ band with the incorporation of Nd, Mg and (Mg + Nd) ions while the area of the $E(TO_8)$ band remains approximately constant. Thus the general tendency of the area ratio of the $A_1(TO_4)/E(TO_8)$ bands is to increase. This is shown in figure 3(b).

The $E(TO_1)$ mode consists of Nb vibrations against oxygen ions, just as the $A_1(TO_1)$ and $E(TO_3)$ modes, as was mentioned above for the spectra obtained in the *Y* direction of the single-crystals. In addition, the $E(TO_7)$ mode is attributed to Li/O vibrations. The Raman shift of the $E(TO_1)$ and $E(TO_7)$ modes shows a linear increase with the incorporation of Nd, Mg and (Mg + Nd) ions. Therefore, for large (Mg + Nd) content, the increase of $E(TO_1)$ and $E(TO_7)$ Raman shifts reveals the substitution of Mg and Nd ions for Nb ions. For low (Mg + Nd) concentration, the decrease of $A_1(TO_1)$ and $E(TO_7)$ Raman shift is not in contradiction with the fact that more Nb sites are occupied by Nb ions, which are pushed out from Li sites by Nd and (Mg + Nd) ions, and thus reflects a change in the doping process. This is shown in figures 5(a) and (b).

In consequence, we can clearly define two ranges of general tendency in the (Mg + Nd) doping mechanism: (i) range I; for (Mg + Nd) concentrations smaller than approximately 5 mol% in the crystal, the Mg and Nd ions are located on the Li sites only. (ii) Range II; for (Mg + Nd) content larger than approximately 5 mol%, the Mg and Nd ions are lying in both Li and Nb sites. Furthermore, we have some indications about the three different kinds of Li sites, since the increasing of (Mg + Nd) doping produces the substitution of Mg and Nd ions for Nb_{Li}, V_{Li} (in range I) and Li_{Li} (in range II).

The concentration dependence of the half-width for modes $E(TO_1)$ and $E(TO_7)$ can be interpreted in terms of some ordering occurring in the LN lattice, according to the above description of the Mg and Nd substitution dynamics. Indeed, the damping of TO_1 and TO_7 mainly reflects the order in the Nb and Li sites respectively. In range I, Mg and Nd substitution of unstable Nb_{Li} and V_{Li} in an empty and thus deformable octahedron favors an ordering process.

For higher concentrations, i.e. in the range II, the Li ion substitution by Mg and Nd ions causes a large disorder of the Li sites whereas the order in the Nb sites is unaffected by a partial replacement of Nb ions by Mg and Nd ions. For low (Nd + Mg) concentrations, sites deficient in lithium have already been occupied by them and for high concentrations they start occupying the Nb sites, affecting the neighboring Li sites.

4. Conclusions

We have discussed the mechanisms of Nd and Mg ions' incorporation in the LN lattice in the light of recent lattice dynamical calculations, as well as from the Raman data recorded in the *Y* and *Z* directions of the single-crystals with varying Nd and Mg ion concentrations. It was pointed out that there are two general tendencies of the (Mg + Nd) concentration ranges that can be established according to their effects. In range I for (Mg + Nd) content smaller than approximately 5 mol%, Mg and Nd ions lie in the Li sites and substitute niobium antisites and Li vacancies. These processes contribute to an increasing ordering of the lattice. In range II, for (Mg + Nd) concentrations larger than approximately 5 mol%, Mg and Nd ions replace both Li and Nb ions on their own sites. The present interpretation is independent of the defect model chosen to describe the undoped crystal.

Acknowledgments

This work was partially supported by DGEP-UNAM (México). We gratefully acknowledge the grant support from Centro Latino-Americano de Física (CLAF), PFAMU-UNAM program and CONACYT (México) with project No. J51441-F. The authors are grateful to A Ródenas for helping us in the experimental measurements. We are also grateful to E Cantelar for providing us with one of the single-crystals used in this study. The authors thank Dr C García Segundo for revision of the manuscript and Mr D Murrieta F for assistance with the English.

References

[1] Bryan D A, Gerson R and Tomasche H E 1984 *Appl. Phys. Lett.* **44** 847

[2] Furukawa Y, Kenji K, Shunji T, Kazuo N and Hideki H 1998 *Opt. Lett.* **23** 1892

[3] Lifante G, Cussó C, Jaque F, Sanz-García J, Monteil A, Varrel B, Boulon G and García Solé J 1991 *Chem. Phys. Lett.* **176** 482
[4] Tocho J O, Sanz García J A, Jaque F and García Solé J 1991 *J. Appl. Phys.* **70** 5582
[5] Burlot R, Moncorgé R, Manaa H, Boulon G, Guyot Y, Garcia Solé J and Cochet-Muchy D 1996 *Opt. Mater.* **6** 313
[6] García-Solé J, Petit T, Jaffrezic H and Boulon G 1993 *Europhys. Lett.* **24** 719
[7] Lorenzo A, Loro H, Muñoz Santiuste J E, Terrible M C, Boulon G, Bausá L E and García Solé J 1997 *Opt. Mater.* **8** 55
[8] Postnikov A V, Caciuc V and Borstel G 1999 *J. Phys. Chem. Solids* **61** 295
[9] Repelin Y, Husson E, Bennani F and Proust C 1999 *J. Phys. Chem. Solids* **60** 819
[10] Caciuc V, Postnikov A V and Borstel G 2000 *Phys. Rev.* B **61** 8806–13
[11] Ridah A, Bourson P, Fontana M D and Malovichko G 1997 *J. Phys.: Condens. Matter* **9** 9687
[12] Ridah A, Fontana M D and Bourson P 1997 *Phys. Rev.* B **56** 5967
[13] Abrahams S C and Marsh P 1986 *Acta Crystallogr.* B **42** 61
[14] Lengyel K, Kovács L, Péter Á, Polgár K and Corradi G 2007 *Appl. Phys.* B **87** 317
[15] Lengyel K, Kovács L, Péter Á, Polgár K, Corradi G and Bourson P 2007 *Phys. Status Solidi* c **3** 847
[16] Kong Y, Xu J, Chen X, Zhang C and Zhang W 2000 *J. Appl. Phys.* **87** 4410
[17] Sidorov N V, Chufyrev P G, Palatnikov M N, Mel'nik N N and Kalinnikov V T 2005 *Inorg. Mater.* **41** 164
[18] Mouras R, Bourson P, Fontana M D and Boulon G 2001 *Opt. Commun.* **197** 439
[19] Donnerberg H 1996 *J. Solid State Chem.* **123** 208
[20] Kim I W, Moon B G, Jeong J J, Park H L and Pichugin V F 2001 *Mater. Lett.* **49** 324
[21] Mouras R, Fontana M D, Bourson P and Postnikov A V 2000 *J. Phys.: Condens. Matter* **12** 5053
[22] Wu S-Y and Dong H-N 2005 *J. Alloys Compounds* **386** 52